Journal of Fluorine Chemistry 130 (2009) 1080–1085

Contents lists available at ScienceDirect

Journal of Fluorine Chemistry

journal homepage: www.elsevier.com/locate/fluor

Study of the fluorination of carbon anode in molten KF-2HF by XPS and NMR investigations

I. Crassous [a], H. Groult [a,*], F. Lantelme [a], D. Devilliers [a], A. Tressaud [b], C. Labrugère [b], M. Dubois [c], C. Belhomme [d], A. Colisson [d], B. Morel [d]

[a] UPMC Univ Paris 06, UPMC-ESPCI-CNRS UMR 7195, Laboratoire PECSA, 4 Place Jussieu, Paris F-75005, France
[b] Institut de Chimie de la Matière Condensée de Bordeaux ICMCB-CNRS, Université Bordeaux 1, 87 Av Dr. A. Schweitzer, 33608 PESSAC Cedex, France
[c] Clermont Université, Université Blaise Pascal, Laboratoire des Matériaux Inorganiques – CNRS UMR 6002, 24, avenue des landais, 63177 Aubière Cedex, France
[d] AREVA/Comurhex, Laboratoire R&D, BP 29, 26701 Pierrelatte Cedex, France

ARTICLE INFO

Article history:
Received 8 May 2009
Received in revised form 20 July 2009
Accepted 21 July 2009
Available online 21 August 2009

Keywords:
Fluorine
KF-2HF
XPS
NMR
Carbon

ABSTRACT

During the electrolysis of molten KH-2HF, a solid CF film is formed on carbon anodes. The influence of the potential applied to the anode on the composition of the CF surface film was studied by XPS and NMR. Results obtained with carbon electrochemically passivated in molten KF-2HF have been compared with those obtained with carbon simply immersed in molten KF-2HF without any polarization. Whatever the potential, and even in the case of carbon sample immersed in molten KF-2HF without any polarization, the presence of covalent and semi-ionic C–F bonds has been pointed out both by XPS and NMR. For polarized samples, the higher the potential applied to the anode in KF-2HF, the higher the fluorination level. From investigations carried out with carbon activated at 40 V in molten KF-2HF, it was concluded that the electropolishing of the surface induced by this treatment allows enhancing drastically the fluorine evolution reaction.

1. Introduction

Fluorine gas is produced by electrolysis of molten KF-2HF on carbon anodes [1–11]. During this process, a thin fluorocarbon layer (denoted CF) is formed on the carbon surface and the high anodic overvoltage which characterizes the fluorine evolution reaction (FER) is mainly due to the presence of such a CF film [1–17]. This process is also characterized by the peculiar properties of F_2 bubbles which have a lenticular shape and are strongly adherent to the surface. These features result in a limitation of the electroactive surface area. The contact angles are obviously influenced not only by the interfacial tension according to the Young's equation but also by other parameters such as the roughness and the surface heterogeneity. Thus, the shape of F_2 bubbles is intimately linked to the nature and the chemical composition of the surface CF film. During the last decade, one of our objectives has been to improve the process, i.e. to enhance the FER. Among the different parameters which can influence the FER, the knowledge of the chemical composition of CF is required. In that goal, several investigations have been carried out. STM analyses performed on HOPG samples fluorinated in molten KF-2HF [4,16] have pointed out the presence of conducting areas attributed to fluorine-graphite intercalation compounds (noted F-GICs) having the same hexagonal symmetry as raw HOPG. In these F-GICs, the positive charge is delocalized on several carbons [18] and these compounds are well known to be conductive and wetted by molten KF-2HF. Traces of insulating graphite fluorides (denoted CF_x) were also suggested to be present in many parts of the electrode since no current was detected in some areas, no image was collected in spite of very high imposed bias values. XPS measurements have confirmed that the CF film formed on the anode materials is composed of conductive fluorine-GICs with semi-ionic C–F bonds and insulating CF_x with covalent C–F bond [19]. Finally, AFM investigations coupled with local electrical measurements in ambient air on HOPG fluorinated in molten KF-2HF [4,19] have allowed to valid the presence of these two kinds of areas onto the surface. Thus, we have been able to propose a schematic representation of the surface after passivation in molten KF-2HF: the surface can be assimilated to a leopard skin with conducting and insulating compounds. Consequently, the fluorine evolution reaction (FER) should occur mainly at the surface of conducting areas covered by F–GICs due to the insulating properties of the CF_x.

All these investigations mostly dealt with the characteristic CF film formed at high potential in molten KF-2HF. In the present study, we focus our attention on the influence of the potential

* Corresponding author. Tel.: +33 1 4427 3534; fax: +33 1 4427 3856.
E-mail address: henri.groult@upmc.fr (H. Groult).

0022-1139/$ – see front matter © 2009 Elsevier B.V. All rights reserved.
doi:10.1016/j.jfluchem.2009.07.022

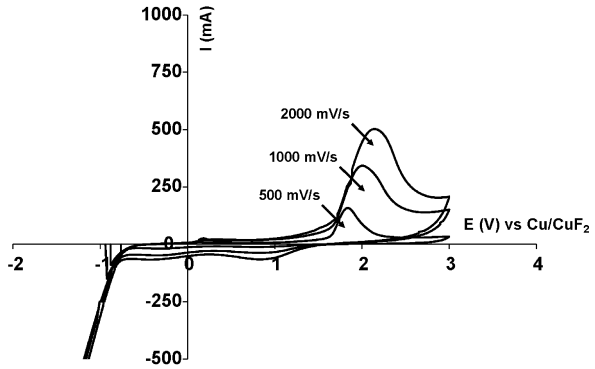

Fig. 1. *I–E* curves obtained in molten KF-2HF at 90 °C with sample 0 for different scan rates. $S = 2\ cm^2$.

applied to the carbon anode in molten KF-2HF on the CF surface film composition. Indeed, the passivation of carbon in molten KF-2HF starts at low potential, i.e. before the fluorine evolution [20]. Therefore, the CF film formation will be studied in a large potential window from 2.5 to 40 V. The obtained results will be compared with those of raw carbon anode simply immersed in molten KF-2HF. To succeed, electrochemical tests by cyclic voltammetry and impedance will be coupled with NMR and XPS analyses.

2. Results

2.1. Electrochemical tests in molten KF-2HF

Current–potential curves were recorded in molten KF-2HF for different potential windows. The curves obtained between 0 and 3.0 V for different scan rates and between 3 and 6 V are presented in Figs. 1 and 2, respectively.

The peak observed in Fig. 1 at around 2 V vs Cu/CuF_2 is related to the passivation of the carbon electrode, i.e. the formation of a solid fluorocarbon film at the surface of the electrode [1–20]. Such a fluorocarbon film could result from the presence of a small amount of water in molten KF-2HF and/or the presence of different kinds of C–O bonds at the carbon surface. In the presence of water, and in addition with O_2, CO, CO_2, COF_2 and F_2O evolution in the anodic compartment, graphite oxide can be formed [2,4,6,19] at low potential (<3 V) according to the following reaction:

$$zC + (y+1)H_2O \rightarrow C_zO(OH)_y + (y+2)H^+ + (y+2)e^- \quad (1)$$

At higher potentials, oxygen intercalated in graphite oxide, $C_zO(OH)_y$, may be easily exchanged with fluorine to form insulating graphite fluoride [2,4,6,19]:

$$C_zO(OH)_y + (2 + zx + 3y)F^- \rightarrow zCF_x + (1+y)F_2O + yHF + (2 + zx + 3y)e^-$$

This reaction is concomitant with the formation of fluorine gas which is described by the following half cell reaction:

$$HF_2^- \rightarrow 1/2F_2 + HF + e^- \quad (3)$$

Reaction (3) is strongly limited on graphite fluorides because of their insulating properties [19]. It occurs mainly on the parts of the electrode resulting from the electrofluorination of carbon. On those parts, HF_2^- species are electrochemically intercalated into the carbon lattice according to:

$$xC + HF_2^- + (y-1)HF \rightarrow C_x(HF)_yF + e^- \quad (4)$$

In these $C_x(HF)_y$ F-GICs, the positive charge is delocalized on x carbons. Moreover, this compound is well known to be conductive and wetted by molten KF-2HF [2,4]. The presence of such conductive compounds can explain why the current does not reach a null value after the passivation peak, as usually observed in the case of insulating thin film formation.

During the reverse scan (Fig. 1), the cathodic limit corresponds to H_2 evolution. Two weak reduction peaks were observed at around +0.80 and −0.45 V vs Cu/CuF_2 which can be attributed to the reduction of the CF compounds formed during the passivation process. It can be noticed that the intensities of the reduction peaks do not increase significantly with increasing sweep rate as it is observed for the anodic peak. It is well known that the formation of fluorocarbon CF_x in such conditions is an irreversible process [20]. Therefore, one may assume that the oxidation peak results from the formation of both CF_x and F-GICs whereas the reduction peaks imply only the reduction of the F-GICs. Finally, it must be noted that the intensity of the reduction peak should be larger in the case of graphitised carbon anodes since the hexagonal structure favours the formation of larger amount of F-GICs [20].

Fig. 2 gives the voltammograms obtained with samples 3 and 4 [19]. This figure clearly shows that a pre-treatment of the carbon surface by activation at 40 V (sample 4) significantly increases the kinetics of the fluorine evolution reaction. In other words, for a same current density, a higher voltage is required to produce the same amount of fluorine when the carbon is not activated prior to electrolysis (sample 3). Thus, the activation process induces a significant decrease of the anodic overvoltage. The effect of activation procedure on the kinetics rate of the FER was evidenced by impedance measurements performed with samples 3 and 4. For instance, the impedance diagrams obtained in the Nyquist representation at 4.2 V vs Cu/CuF_2 are presented in Fig. 3.

As shown in this figure, the charge transfer resistance which is approximately given by the diameter of the semi-circle is much more lower in the case of an activated carbon electrode (sample 4) than that observed in the case of a carbon electrode passivated at 6 V (sample 3), indicating a faster kinetics in the case of activated carbon electrodes.

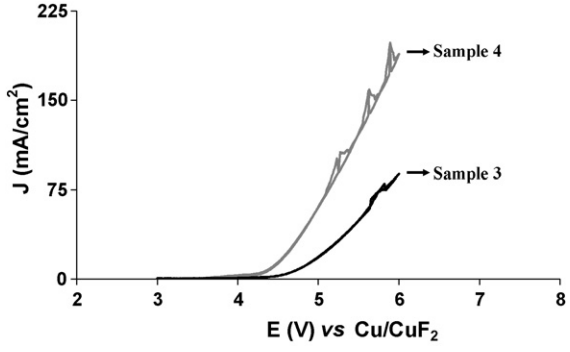

Fig. 2. *I–E* curves ($v = 0.4\ V\ s^{-1}$) obtained in molten KF-2HF at 90 °C with samples 3 and 4 [19].

2.2. Physical-chemical characterizations

2.2.1. XPS

2.2.1.1. Reference carbon sample. First, raw carbon electrode (Sample 0) was studied in order to identify the basic hydrogenated and/or oxygenated sites. Individual fitted parameters (binding energy, BE), as well as the relative contribution of each component (I_i/%) to the total area under the peak are calculated for the different groups. The C1s photoelectron peak (Fig. 4) can be decomposed in

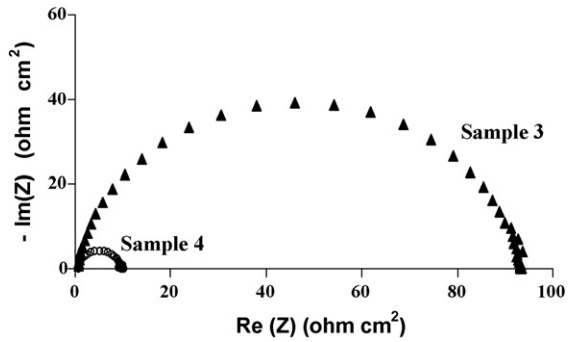

Fig. 3. Impedance diagrams obtained in the Nyquist representation for samples 3 and 4 performed in molten KF-2HF at 4.2 V vs Cu/CuF_2 [4].

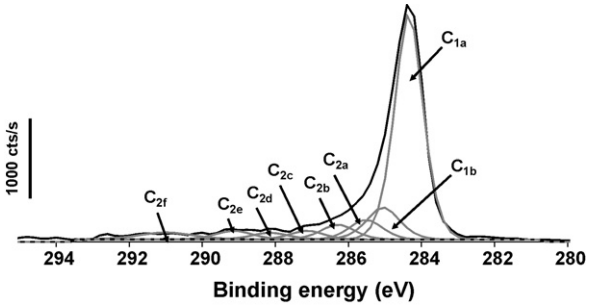

Fig. 4. C1s XPS spectrum of pristine electrode (sample 0).

eight symmetrical peaks denoted C_{1a}, C_{1b}, C_{2a}, C_{2b}, C_{2c}, C_{2d}, C_{2e} and C_{2f} situated at 284.3, 285.0, 285.5, 286.3, 287.1, 288.1, 289.1 and 291.0 eV, respectively.

The peaks denoted C_{1a} and C_{1b} located at around 284.3 and 285.0 eV correspond to non-functionalized C(sp^2) and C(sp^3) atoms, respectively, which have not been affected by fluorination. The area of these two components represents 76% of the total area of the C1s envelope (Table 1).

The additional peaks denoted C_{2a} to C_{2e} are due to C–CO, C–O, C=O, COOR and COOH, respectively. As mentioned above, the presence of such oxygenated bonds could be very important during the fluorination process of the carbon surface in molten KF-2HF with or without fluorine evolution. The surface oxygen content deduced from the survey analysis is about 8%.

2.2.1.2. Carbon anode dipped in molten KF-2HF without any polarization. A raw carbon anode was dipped in molten KF-2HF during 40 days without any polarization (sample 1) in order to study the changes in the surface composition. The detailed analysis of the high resolution C1s spectrum is given in Fig. 5.

Table 1
XPS data for raw carbon electrode (sample 0). C1s binding energy, BE, and relative amounts of different components I_i.

Component	Sample 0		Assignment
	BE (eV)	I_i (%)	
C_{1a}	284.3	65	C(sp^2)
C_{1b}	285.0	11	C(sp^3)
C_{2a}	285.5	5	C–CO
C_{2b}	286.3	2	C–O
C_{2c}	287.1	2	C=O
C_{2d}	288.1	3	COOR
C_{2e}	289.1	4	COOH
C_{2f}	291.0	5	π–π*

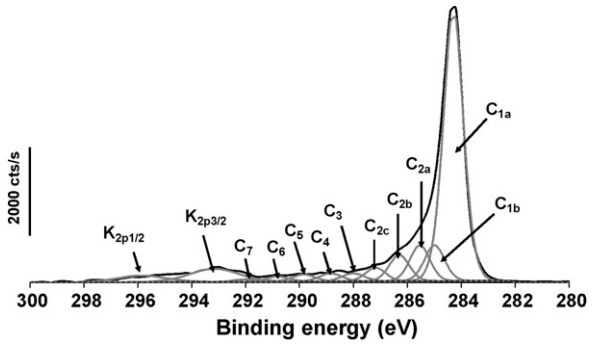

Fig. 5. C1s XPS spectrum of sample 1.

The individual fitted parameters (binding energy, BE), as well as the relative contribution of each component (I_i/%) to the total area are compiled in Table 2.

The C1s photoelectron peaks can be fitted into several symmetrical peaks. Besides the contribution of potassium K2p present on the film, several contributions were considered to fit the experimental curve [21–25]. The peaks denoted C_{1a} and C_{1b} located at around 284.3 and 285.0 eV correspond to non-functionalized C(sp^2) and C(sp^3) atoms, respectively, which have not been affected by fluorination. The area of these two components represents 74% of the total area of the C1s envelope for sample 1. The peaks C_{2a}, C_{2b} and C_{2c} at around 285.5, 286.3 and 287.2 eV, respectively, are due to C atom bound to O (peaks C_{2a}, C_{2b} and C_{2c}) and/or to carbon atom not directly bound to F atom but having CF_n next neighbours. The C_3 peak at 288.0 corresponds to C–F bonding in $\underline{C}HF–CH_2$ or $\underline{C}HF–CHF$ units and semi-ionic bonding (fluorine intercalated in graphitic domains), whereas the C_4 peak at 288.8 eV is related to C–F bonding in more fluorinated environments $\underline{C}HF–CF_2$ and $\underline{C}F_x–CF–CF_{x'}$ with (x, x' = 2, 3). The peaks C_5 and C_6 located at around 289.8 and 290.8 eV, respectively, are assigned to CF_2 groups in $\underline{C}F_2–CH_2$ and $\underline{C}F_2–CHF$ units. Finally, the C_7 peak observed at 292.0 corresponds to PTFE-like $CF_2–CF_2$ units.

To summarize, a simple contact between the carbon anode and molten KF-2HF leads to the fluorination of the surface; the CF film formed during this process is characterized by the presence of different kinds of C–F bonds. The F surface content deduced from the survey spectra is about 12.6%; it means that the fluorination of the surface is effective by only a simple immersion of the electrode in molten KF-2HF and without any polarization.

The surface fluorination should not result from the direct interaction between F and C because such a process suggests the modification of the hybridized state of the carbon which requires a large overvoltage. In addition, TEM observations have evidenced the complex morphology of such carbon which is composed of nanometric graphitic domains [19]. Consequently, the fluorination mechanism should be compared with the one observed for carbon blacks [25]. In this fluorination process, the first step (type I) occurs on specific sites at the periphery of graphitic domains notably where C–O bonds are present. Nevertheless, one cannot neglect the potential role of oxygen-free edges sites present also at the periphery of graphene sheets [26]; their concentration is expected to be quite high in comparison to the basal planes sites and could also contribute to the formation of C–F bonds. The second fluorination step (type II) corresponds to the formation of perfluorinated structures mostly composed of CF groups [21–23].

2.2.1.3. Carbon anodes polarized at 2.5 and 6 V in molten KF-2HF. Carbon anodes were then polarized in molten KF-2HF at different potentials (2.5 V for sample 2 and 6 V for sample 3) and

Table 2
XPS data for samples 1–3. C1s binding energy, BE, and relative amounts of different components I_i.

Component	Sample 1		Sample 2		Sample 3		Assignment
	BE (eV)	I_i (%)	BE (eV)	I_i (%)	BE (eV)	I_i (%)	
C_{1a}	284.3	65.4	284.3	53.0	284.2	21	Non-functionalized C(sp^2) atoms non-affected by fluorination
C_{1b}	285.0	8.6	285.0	6.7	285.0	4.7	Non-functionalized C(sp^3) atoms non-affected by fluorination
C_{2a}	285.5	8.5	285.3	12.4	285.7	8.1	C–CO and/or C–(CH_2–CF_x)
C_{2b}	286.3	6.2	286.2	8.6	286.6	6.9	C–O and/or CH_2–CHF
C_{2c}	287.2	3.3	287.0	4.4	287.6	7.0	C=O and/or CH_2–CF_2
C3	288.0	2.1	287.9	4.4	288.4	10.5	CHF–CH_2 and CHF–CHF; semi-ionic C–F (intercalation)
C_4	288.8	1.9	288.9	6.6	289.3	18.8	CHF–CF_2 and CF_x–CF–$CF_{x'}$ with (x, x' 2, 3) in type I domains
C_5	289.8	1.9	289.7	1.4	290.4	5.5	CF_2–CH_2; CF groups of type I structure next neighbours to CF_n groups
C_6	290.8	1.4	290.9	1.5	291.2	8.7	CF_2 groups of type I domains and CF groups of type II domains
C_7	292.0	0.7	292.3	1.0	292.4	4.2	CF_2–CF_2 groups
C_8	–	–	–	–	293.3	3.7	CF_2–CF_3
C_9	–	–	–	–	294.3	1.1	CF_3 groups in highly fluorinated environment
I (C_{1a}+C_{1b})	0.74		0.60		0.26		

analysed by XPS. As an example, the C1s region obtained for sample 2 polarized at 2.5 V during 20 days is given in Fig. 6.

The individual fitted parameters (binding energy, BE), as well as the relative contribution of each component (I_i/%) to the total area for samples 2 and 3 are compiled in Table 2. The contribution of the C_{1a} and C_{1b} peaks related to non-functionalized C(sp^2) and C(sp^3) atoms drastically decreases with increasing voltage: in the case of sample 1 (no polarization), the area of these two components represented 74% of the total area of the C1s envelope, whereas this amount is about 60% for sample 2 (polarized at 2.5 V) and only 26% for sample 3 (polarized at 6 V). The increase of the applied potential to the electrode in KF-2HF seems to give thicker CF surface films. Among the different peaks used for the fitting of the C1s envelope, one can point out the increase of the C_4 peak located at around 288.9 eV. This peak is notably assigned to C atom covalently linked to F atom as found in insulating graphite fluorides [1]. The area of this component represents 19% of the total area of the C1s envelop in the case of sample 3, a value much higher than those observed in sample 1 (1.9%) and sample 2 (6.6%). It means, the higher the potential applied to the electrode in molten KF-2HF, the higher the resistivity of the CF surface film. This is confirmed by the occurrence of the two peaks C_8 and C_9 at 293.3 and 294.1 eV related to the presence of CF_3 groups. However, it should be noted that the presence of K2p peaks hinders a good fitting for these high BE C1s peaks. Thus, the CF film generated on sample 3 should be slightly more insulating than the one formed on samples 1 and 2.

The survey spectra analysis has shown that the F surface contents are about 28% for sample 2 and about 45% for sample 3, confirming the higher fluorination level of the carbon surface for higher applied voltage.

2.2.1.4. Carbon anodes polarized at 40 V in molten KF-2HF. Finally, the results presented above have been compared with those obtained with a carbon anode polarized at 40 V during 1 min (sample 4). As reported in a previous paper [4,19], this treatment (called activation) modifies drastically the morphology of the carbon surface. Two different areas have been distinguished on SEM images [19]: for the first one, no significant difference appears in the texture with respect to the raw carbon surface. These areas will be called "rough" areas hereafter. For the second one, a smoothing and a cleaning of the electrode have been induced by activation. These areas will be called "mirror-like" areas henceforth. The presence of the latter could strongly facilitate the detachment of fluorine bubbles from the surface by reducing the contact angle. These two different areas have been analysed by XPS. Individual fitted parameters (BE), as well as the relative contribution of each component to the total area under the peak are presented in Table 3.

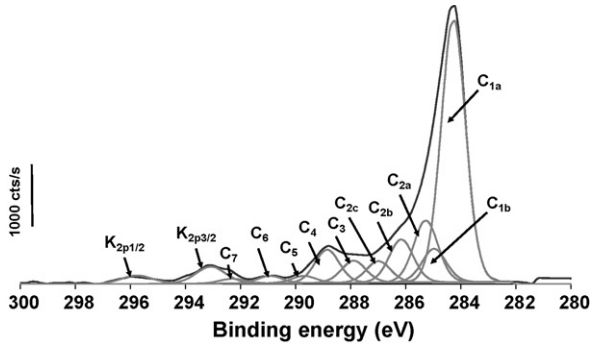

Fig. 6. C1s XPS spectrum of sample 2.

The areas relative to the two C_{1a} and C_{1b} peaks represent about 32% of the total area of the C1s envelope for the "mirror-like" areas and 39% for the "rough" areas. These values are slightly higher than those obtained with sample 3 (26%) indicating the presence of a thinner CF layer onto the carbon anode in the case of sample 4. However, whatever the studied areas, the activation procedure leads to the formation of a CF film with a higher fluorinated degree illustrated by the presence of C_8 and C_9 peaks relative to CF_3 groups. So, the CF film in the case of sample 4 is thinner but has a higher F content. We considered also the ratio, r, equal to $\sum IC_i/I_{tot}$ (with i = 3–9) that is the ratio of the area of the components relative to carbon atoms directly linked to F atoms (peaks C_3–C_9) to that of the total area ($I_{tot} = \sum IC_j$ with j = 1–9). We found that r equals 0.08 (sample 1), 0.15 (sample 2) and 0.53 (sample 3). For sample 4, r = 0.55 for the "mirror-like" areas and r = 0.37 for the "rough" areas. The trend clearly accounts for the increase of fluorine contents with polarization voltage. The values of r ratios for the mirror-like and rough domains evidence higher fluorine content in the former type with simultaneous lower amounts of contamination and oxidized carbon. Consequently, one can assume that the improvement of the FER observed with sample 4 (see Figs. 2 and 3) should be mainly due to the electropolishing of the surface induced by the activation procedure and as pointed out by SEM [19]. This electropolishing facilitates the F_2 detachment from the surface. Such a positive effect of the polishing of carbon anodes on the FER has been already reported in the literature [27].

2.2.2. NMR characterizations

To complete the XPS results presented above, NMR investigations have been carried out with samples 1–4. The room temperature ^{19}F MAS NMR spectra at spinning rate of 10.0 kHz are displayed in Fig. 7 for the samples.

High resolution solid state NMR is a well adapted technique for the study of graphite fluorides [28–32] and fluorine-graphite

Table 3
XPS data for sample 4. C1s binding energy, BE, and relative amounts of different components I_i.

	Sample 4				Assignment
	Mirror-like areas		Rough areas		
	BE (eV)	I_i (%)	BE (eV)	I_i (%)	
C_{1a}	284.3	28.2	284.3	27.0	Non-functionalized C(sp^2) atoms non-affected by fluorination
C_{1b}	285.0	4.3	285.0	12.2	Non-functionalized C(sp^3) atoms non-affected by fluorination
C_{2a}	285.5	4.6	285.5	8.0	C–CO and/or C–(CH_2–CF_x)
C_{2b}	286.3	5.1	286.3	8.0	C–O and/or CH_2–CHF
C_{2c}	287.3	2.8	287.3	7.8	C=O and/or CH_2–CF_2
C_3	288.2	15.0	288.2	5.8	CHF–CH_2 and CHF–CHF; semi-ionic C–F (intercalation)
C_4	289.3	17.2	289.2	11.1	CHF–CH_2 and CF_x–CF–$CF_{x'}$ with (x, x' = 2, 3) in type I domains
C_5	290.4	5.9	290.4	5.2	CF_2–CH_2; CF groups of type I structure next neighbours to CF_n groups
C_6	291.2	10.1	291.3	2.7	CF_2 groups of type I domains and CF groups of type II domains
C_7	292.2	4.0	292.4	2.6	CF_2–CF_2 groups
C_8	293.2	2.9	293.5	4.3	CF_2–CF_3
C_9			294.5	5.3	CF_3 groups in highly fluorinated environments
I (C_{1a} + C_{1b})	0.33		0.39		

intercalation compounds (F-GICs) [28,33,34]. It makes possible to specifically study the intercalated species (considering ^{19}F or ^{1}H nucleus) for their identification or the fluorocarbon matrix (^{19}F and ^{13}C). Moreover, the nature of the interactions between carbon and fluorine atoms informs about the C–F bonding which can be classified in two categories: covalent and ionic. This bonding results in different ^{19}F chemical shifts (denoted $\delta_{^{19}F}$): the higher the covalence, the lower the chemical shift. For instance, a $\delta_{^{19}F}$ of −190 ppm is measured for covalent $(CF)_n$ [31] and $(C_2F)_n$ [32] types whereas values ranged from −147 to 160 ppm are obtained for semi-ionic room temperature graphite fluoride [28,32–34].

The main lines are marked by dotted lines. Four types of fluorine nuclei with $\delta_{^{19}F}$ of −129, −135, −153 and −170 ppm/$CFCl_3$ are underlined. When the sample is simply immersed in molten KF-2HF without any polarization (sample 1), the resulting spectrum exhibits a first line at −129 ppm assigned to CF_2 groups, in good accordance with the XPS results (Table 2). A second line is also observed at −153 ppm. Taking into account the nature of the electrolyte, i.e. molten KF-2HF, this line could be related to intercalated HF_2^- ions into the carbon lattice according to reaction (4). As a matter of fact, chemical shifts at around −150 ppm have been measured in graphite fluorides synthesized at room temperature using a F_2/HF/(BF_3 or Cl_2) gaseous mixture [35,36]. On the contrary, when non-hydrogenated F^- species are intercalated, e.g. in $(C_{2.5}F)_n$ fluorine-GIC, its $\delta_{^{19}F}$ is equal to −190 ppm

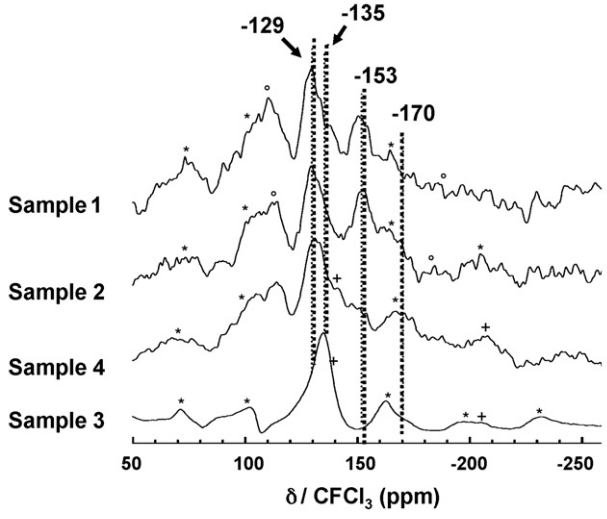

Fig. 7. ^{19}F MAS NMR spectra of polarized samples (spinning speed of 10 kHz). (*) and (°) are the spinning sidebands.

[34]. The contribution of CF_2 and HF_2^- already discussed in the case of sample 1 is also predominant for the sample 2 (polarized at 2.5 V) but two additional lines appear as shoulders at −135 and −170 ppm. To interpret the presence of these two additional bands, interesting information can be extracted from the analysis of the NMR spectra obtained with samples 3 and 4, passivated at higher potential in molten KF-2HF. The high relative intensities observed after polarization at 6.0 V (sample 3) or activation at 40 V (sample 4) suggest the presence of large amount of CF_2 groups giving rise to a chemical shift of −135 ppm. The chemical shifts of CF_2 groups slightly differ for sample 1 ($\delta_{^{19}F}$ = −129 ppm) and sample 3 ($\delta_{^{19}F}$ = −135 ppm). This indicates that the neighbouring of these CF_2 groups is not equivalent. Such groups have been detected by XPS on the surface of all samples, even for non-polarized sample (sample 1). Whereas the contribution of HF_2^- significantly decreases for activated sample 4 and disappears for sample 3, an additional line is also observed for these two last samples at −170 ppm. Therefore, one may suggest that this new band could be assigned to covalent C–F bonds since its chemical shift is comprised in between the values of the fluorocarbon matrix in F-GIC with composition of $(C_{2.5}F)_n$ ($\delta_{^{19}F}$ = −147 ppm) and in graphite fluorides ($\delta_{^{19}F}$ = −190 ppm) for both $(CF)_n$ and $(C_2F)_n$ types). The C–F bonding in the sample 3 exhibits similarities with graphite fluorides prepared at room temperature using F_2(g)/HF(g)/MF_n(g) mixture (MF_n = IF_5, BF_3 or ClF_x); indeed, $\delta_{^{19}F}$ being close to −154 ppm whatever the used catalyst [35–38]. It must be noted that this line is also present for sample 3 but appears as a shoulder of the first spinning sideband of CF_2 lines. The amount of CF_2 groups is higher than for the others samples.

To summarize, this NMR study reveals that in the case of samples 1 and 2, the fluorination results mainly in the intercalation of HF_2^- species. Nevertheless, even for sample 1 which was not polarized in molten KF-2HF, a line with a small intensity assigned to the presence of CF_2 groups has been observed. As soon as a polarization potential of 2.5 V is applied to the electrode (samples 2–4), CF_2 groups and covalent C–F bonds start to be formed. Their amounts significantly increase at 6.0 V (sample 3) whereas HF_2^- are either desintercaled or converted into C–F bonds by reaction with the host matrix. Finally, one must underline the good correlation between the results obtained by XPS measurements and NMR studies even if the NMR analyses concern the overall bulk of the carbon electrode whereas the XPS investigations give information only on the outmost surface.

3. Conclusions

The formation of solid CF film on carbon anodes in molten KF-2HF has been investigated. At first, electrochemical tests were

performed by cyclic voltammetry and impedance measurements. It has been shown that, when a high potential of 40 V is applied to the carbon anode, the anodic overvoltage which characterizes the fluorine evolution process is significantly decreased. Then, physical–chemical characterizations have been performed by XPS and NMR. Results obtained with carbon electrochemically passivated in molten KF-2HF have been compared with those obtained with carbon simply immersed in molten KF-2HF without any polarization. These investigations have shown that the formation of CF film is effective even in the case of the non-polarized sample immersed in molten KF-2HF. Whatever the fluorination procedure, covalent and semi-ionic C–F bonds have been revealed both by XPS and NMR. It has also been pointed out that the higher the potential applied to the electrode in KF-HF, the higher the fluorination level. For carbon activated at 40 V in molten KF-2HF, the CF film is thinner but has a higher fluorine content. Nevertheless, it exhibits the best electrochemical behaviour in molten KF-2HF; this is due to the electropolishing effect on the surface which renders the fluorine evolution easier. Finally, it must be noticed that even if the activation of carbon anode is very attractive in terms of enhancement of the electrochemical performances vs fluorine evolution reaction, it can be realised only at a laboratory-scale and not on large scale electrodes in industrial cells because this procedure is dangerous due to the generation of sparks and heat production which should be eliminated.

4. Experimental details

Electrochemical experiments were carried out under fluorine evolution by electrolysis of dehydrated molten KF-2HF at around 95 °C. A steel auxiliary electrode and a Cu/CuF_2 [4,39] reference electrode (+0.4 V vs $Pt–H_2$) were used. All potential values were referred to this reference. The *I–E* curves were obtained with an EG&G PAR model 273 generator in a large potential range with a linear potential sweep measurement. The ac impedance measurements were performed with a Solartron-Schlumberger 1255 impedance analyser coupled with an EG&G PAR model 273 potentiostat. The amplitude of the sinusoidal perturbation was 10 mV peak-to-peak; the frequency range was 1 MHz to 1 Hz. The raw anodic material was non-graphitised carbon for fluorine production. Different fluorination procedures were studied:

- raw carbon anode (sample 0) immersed in molten KF-2HF during 40 days without any polarization (giving rise to sample 1);
- raw carbon polarized at 2.5 V during 20 days (sample 2), at 6 V during 7 days (sample 3) or at 40 V during 1 min (sample 4) in molten KF-2HF.

XPS measurements were done with a VG 220 *i*-XL ESCALAB spectrometer under ultrahigh vacuum conditions. The radiation was an Al monochromatized source (1486.6 eV). Silver $Ag3d_{5/3}$ at the binding energies BE = 368.2 eV was chosen for the calibration of the spectrometer. Survey and high resolution spectra were recorded, then fitted with an Avantage processing program provided by Thermo Electron. Each C1s and F1s component was considered as having similar full-width-at-half-maximum (FWHM) for all samples.

^{19}F NMR experiments were carried out with Bruker Avance spectrometer with working frequency of 282.2 MHz. A Magic Angle Spinning (MAS) probe (Bruker) operating with a 4 mm rotor was used. For MAS spectra, a simple sequence was performed with a single $\pi/2$ pulse length of 4.0 μs. Chemical shifts were externally referenced to $CFCl_3$.

References

[1] D. Devilliers, M. Vogler, F. Lantelme, M. Chemla, Anal. Chim. Acta 153 (1983) 69–82.
[2] N. Watanabe, T. Nakajima, H. Touhara, Anode effect in molten fluorides, Graphite Fluorides, vol. 8, Elsevier, Amsterdam, 1988 , pp. 1–22 (chapter 1).
[3] A.J. Rudge, in: A.T. Kuhn (Ed.), Production of Elemental Fluorine by Electrolysis, Industrial Electrochemical Process, Amsterdam, 1971 , pp. 1–69 (chapter 1).
[4] H. Groult, C. Simon, A. Mantoux, F. Lantelme, T. Turq, in: T. Nakajima, H. Groult (Eds.), Fluorinated Materials for Energy Conversion, Elsevier, Amsterdam, 2005 , pp. 1–29 (chapter 1).
[5] H. Groult, J. Fluorine Chem. 119 (2003) 173–189.
[6] D. Devilliers, M. Chemla, in: T. Nakajima (Ed.), Fluorine–Carbon and Fluoride–Carbon Materials, M. Dekker, New York, 1995 , pp. 283–331 (chapter 8).
[7] O.R. Brown, Electrochim. Acta 25 (1980) 367–368.
[8] H. Imoto, T. Nakajima, N. Watanabe, Bull. Chem. Soc. Jpn. 48 (1975) 1633–1634.
[9] L. Bai, B.E. Conway, J. Appl. Electrochem. 18 (1988) 839–848.
[10] M. Jaccaud, R. Faron, D. Devilliers, R. Romano, Ulmann's Encyclopedia of Industrial Chemistry, vol. A11, VCH, Weinheim, 1988, p. 293.
[11] W.V. Childs, G.L. Bauer, J. Electrochem. Soc. 142 (1995) 2286–2290.
[12] H. Groult, D. Devilliers, F. Lantelme, J.-P. Caire, M. Combel, F. Nicolas, J. Electrochem. Soc. 149 (2002) E485–E492.
[13] H. Groult, F. Lantelme, J. Electrochem. Soc. 148 (2001) E13–E18.
[14] F. Lantelme, H. Groult, C. Belhomme, B. Morel, F. Nicolas, J. Fluorine Chem. 127 (2006) 704–707.
[15] H. Groult, D. Devilliers, M. Vogler, C. Hinnen, P. Marcus, F. Nicolas, Electrochim. Acta 38 (1993) 2413–2421.
[16] H. Groult, D. Devilliers, S. Durand-Vidal, F. Nicolas, M. Combel, Electrochim. Acta 44 (1999) 2793–2803.
[17] F. Lantelme, H. Groult, J. Electrochem. Soc. 151 (12) (2004) D121–D126.
[18] T. Nakajima, in: T. Nakajima (Ed.), Fluorine–Carbon and Fluoride–Carbon Materials, M. Dekker, New York, 1995 , pp. 1–31 (chapter 1).
[19] H. Groult, F. Lantelme, I. Crassous, C. Labrugère, A. Tressaud, C. Belhomme, B. Morel, J. Electrochem. Soc. 154 (2007) C331–C338.
[20] D. Devilliers, Thesis P & M Curie University, Paris, 1984.
[21] G. Nansé, E. Papirer, P. Fioux, F. Moguet, A. Tressaud, Carbon 35 (1997) 175–194.
[22] G. Nansé, E. Papirer, P. Fioux, F. Moguet, A. Tressaud, Carbon 35 (1997) 371–388.
[23] G. Nansé, E. Papirer, P. Fioux, F. Moguet, A. Tressaud, Carbon 35 (1997) 515–528.
[24] A. Tressaud, E. Durand, C. Labrugère, J. Fluorine Chem. 125 (2004) 1639–1648.
[25] A. Tressaud, E. Durand, C. Labrugère, A.P. Kharitonov, L.N. Kharitonova, J. Fluorine Chem. 128 (2007) 378–391.
[26] L.R. Radovic, B. Bockrathe, J. Am. Chem. Soc. 127 (2005) 5917–5927.
[27] D. Devilliers, B. Teisseyre, M. Vogler, M. Chemla, J. Appl. Electrochem. 20 (1990) 91–96.
[28] A.M. Panich, Synth. Met. 100 (1999) 169–185.
[29] H. Touhara, F. Okino, Carbon 38 (2000) 241–267.
[30] T. Mallouk, B.L. Hawkins, M.P. Conrad, K. Zilm, G.E. Maciel, N. Bartlett, Philos. Trans. R. Soc. Lond. A 314 (1985) 179–183.
[31] J. Giraudet, M. Dubois, A. Hamwi, W.E.E. Stone, P. Pirotte, F. Masin, J. Phys. Chem. B 109 (2005) 175–181.
[32] M. Dubois, J. Giraudet, K. Guérin, A. Hamwi, Z. Fawal, P. Pirotte, F. Masin, J. Phys. Chem. B 110 (2006) 11800–11808.
[33] J. Giraudet, M. Dubois, K. Guérin, C. Delabarre, P. Pirotte, A. Hamwi, F. Masin, Solid State NMR 221 (2007) 131–140.
[34] M. Dubois, K. Guérin, J.-P. Pinheiro, Z. Fawal, F. Masin, A. Hamwi, Carbon 42 (2004) 1931–1940.
[35] J. Giraudet, M. Dubois, K. Guérin, C. Delabarre, A. Hamwi, F. Masin, J. Phys. Chem. B 111 (2007) 14143–14151.
[36] C. Delabarre, K. Guerin, M. Dubois, J. Giraudet, Z. Fawal, A. Hamwi, J. Fluorine Chem. 126 (2005) 1078–1087.
[37] C. Delabarre, K. Guerin, M. Dubois, Z. Fawal, R. Benoit, A. Hamwi, J. Phys. Chem. Solids 67 (2006) 1157–1161.
[38] J. Giraudet, M. Dubois, K. Guérin, J.P. Pinheiro, A. Hamwi, W.E.E. Stone, P. Pirotte, F. Masin, J. Solid State Chem. 178 (2005) 1262–1268.
[39] A. Mimoto, T. Miyazaki, J. Yamashita, S. Nagamine, M. Inaba, A. Tasaka, J. Electrochem. Soc. 153 (2006) D149–D154.